

Medicinal Boxes Recognition on a Deep Transfer Learning Augmented Reality Mobile Application

Danilo Avola¹, Luigi Cinque¹, Alessio Fagioli¹, Gian Luca Foresti²,
Marco Raoul Marini¹, Alessio Mecca¹, and Daniele Pannone¹

¹ Sapienza University

{avola,cinque,fagioli,marini,mecca,pannone}@di.uniroma1.it

² Udine University

foresti@di.uniroma1.it

Abstract. Taking medicines is a fundamental aspect to cure illnesses. However, studies have shown that it can be hard for patients to remember the correct posology. More aggravating, a wrong dosage generally causes the disease to worsen. Although, all relevant instructions for a medicine are summarized in the corresponding patient information leaflet, the latter is generally difficult to navigate and understand. To address this problem and help patients with their medication, in this paper we introduce an augmented reality mobile application that can present to the user important details on the framed medicine. In particular, the app implements an inference engine based on a deep neural network, i.e., a densenet, fine-tuned to recognize a medicinal from its package. Subsequently, relevant information, such as posology or a simplified leaflet, is overlaid on the camera feed to help a patient when taking a medicine. Extensive experiments to select the best hyperparameters were performed on a dataset specifically collected to address this task; ultimately obtaining up to 91.30% accuracy as well as real-time capabilities.

Keywords: Convolutional Neural Network · Deep Learning · Augmented Reality.

1 Introduction

In the last decade, machine learning and deep learning algorithms have become widespread tools to address many computer vision-based problems, including medical imaging analysis [12], person re-identification [11,7], environment monitoring [15,14,8], emotion recognition [10], handwriting validation [3,4], background modeling [2], and video synthesis [5]. Although effective, these methods usually require a large amount of training data which, however, is not always available. To solve this issue, transfer learning approaches are being exploited to retain previous knowledge from different tasks, and reduce the amount of data required to address the new one [31,6]. A paradigm that is proving particularly relevant to the medical field, where sensitive data is generally employed. As a matter of fact, automatic procedures for detection, classification, and analysis

are already being developed [9,24]. What is more, in concert with these diagnosis-related procedures, mobile applications are also being explored to support patients in their daily routine [23,21,28] since, in general, dealing with the medical aspects of life is a challenging task for both medical operators and sick persons. In particular, operators have to manage several, often elder, people with different pathologies throughout the day. To help this category, applications noticing anomalous patterns can provide a huge healthcare boost, as shown in [30], where bed falls are detected even at nighttime to safeguard patients. Regarding the latter, instead, they tend to either forget when to take a medicine or its required dosage, as reported by [22]. Although it is possible to look up these instructions on the internet or the patient information leaflet (PIL), it can be difficult to find the correct information; suggesting that there is a technological gap that can be filled.

On a different yet related note, hardware advances are enabling mobile devices to execute ever increasingly complex deep learning algorithms, leading to many performance improvements in different fields such as mobile biometrics security through face [18,26] and fingerprint [17,25] recognition. Moreover, the improved hardware, in conjunction with optimized libraries, allows augmented reality (AR) techniques to be run smoothly on most mobile phones. In general, AR applications add a semitransparent layer on top of the camera feed to provide the user with more information with respect to what is being framed by the device. This augmented content can then be decided by analyzing the scene, by exploiting markers, or by using GPS coordinates [27]. What is more, this technology can be applied in heterogeneous application fields such as rehabilitation [13,16], art [19,1], or teaching [29], and it is used to make the application more engaging and compelling to the user.

In this paper, to both leverage hardware advances and help people to take a correct medicinal dosage, we present a mobile AR application that recognizes different kinds of medicines from their package, and provides the user with useful information such as its posology or simplified leaflet. In particular, starting from the smartphone camera feed, video frames are sent to an inference engine for classification. Specifically, the engine is based on a deep neural network exploiting the transfer learning paradigm to overcome the limited amount of training data. Finally, AR is employed to present information on the recognized medicine, and enable real-time interactions by the users. To ensure this time constraint, extensive experiments were performed on a dataset specifically collected for this task, so that the best performing model could be used inside the application.

The rest of this paper is organized as follows. Section 2 introduces the AR mobile application and inference engine used to classify medicinal boxes. Section 3 summarizes information on the collected dataset, relevant implementation details, as well as the obtained results. Finally, Section 4 draws some conclusions on the presented work.

2 Background and Method

In this section, we present the proposed AR pipeline used to classify medicinal packages, and provide details on the application interface as well as the underlying inference engine exploiting the transfer learning paradigm.

2.1 Mobile App AR Interface

To provide patients with extra information on a given medicine in real-time, we devised an iOS AR application that rapidly shows the suggested posology as well as more detailed PIL guidelines when prompted. The mobile application was implemented following the common model–view–controller (MVC) design pattern, summarized in Fig. 1, where different software components are organized into one of the MVC roles. Specifically, application logic and operations,

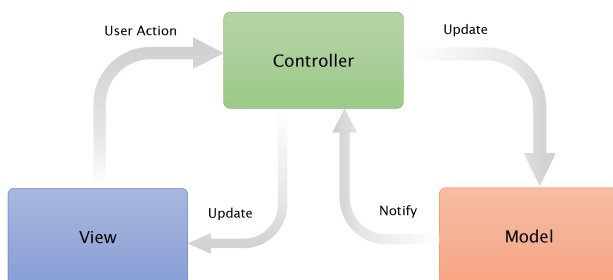


Fig. 1. MVC pattern design scheme.

such as the inference engine, are associated to the model; interface aspects, including rendered AR elements properties, are linked to the view; while the controller is responsible for the data flow between model and view components, allowing for a responsive and well-organized application. By following this pattern, it is possible to develop highly re-usable software and it is easier to extend pre-existing libraries. In particular, we exploited the Apple ARKit framework to implement AR capabilities. In detail, the application controller component sends video frames captured through the mobile device camera to the inference engine and, whenever a medicinal package is recognized, the view component is updated in real-time so that the RGB camera feed is overlaid with meaningful 2D text information, e.g., posology or PIL. Furthermore, the latter are correctly bounded to the corresponding object through the aforementioned framework functionalities; effectively presenting relevant data of a particular medicine to the user. The intuitive AR interface showing either posology or simplified PIL information is reported in Fig. 2.

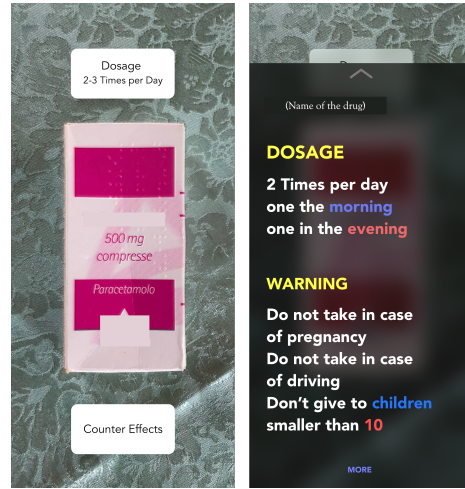


Fig. 2. In-app AR user interface screenshots. On the left, the base overlay showing quick details on the recognized medicine posology. On the right, additional PIL extracted information are instead displayed.

2.2 Inference Engine

To discriminate between medicinal packages and show the correct information inside the AR interface, the application requires a component to perform inference. The latter was implemented as a deep neural network based on transfer learning and imported as the application inference engine via the iOS CoreML framework. In particular, an ImageNet pretrained densenet [20] was selected due to its generally high classification performances as well as its internal architecture. In detail, this network leverages a dense connectivity by introducing links from any layer to any subsequent one, as shown in Fig. 3. Formally, given the

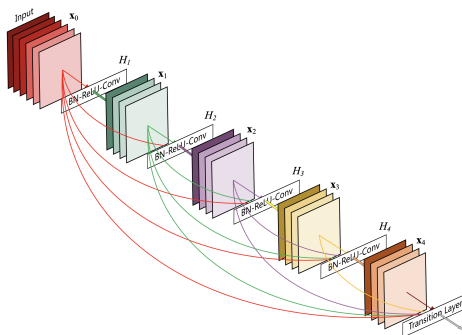


Fig. 3. Densenet dense block scheme. Image courtesy of [20].

l -th layer, its input x_l will be composed by the feature maps of all preceding layers, as follows:

$$x_l = H_l([x_0, x_1, \dots, x_{l-1}]), \quad (1)$$

where $[x_0, x_1, \dots, x_{l-1}]$ represents the concatenation operation of all previous feature maps; while $H_l(\cdot)$ is a composite function applying batch normalization, a rectified linear unit (ReLU) activation function and a 1×1 convolution acting as a bottleneck to consolidate and limit the output size of a given layer. While these dense connections are effective tools to feed-forward information inside a network, they must have the same size in order to be concatenated through Eq. (1). However, this aspect collides with the essential downsampling procedure of a CNN. Therefore, to address this issue, the authors organized their architecture into dense blocks. What is more, transition layers were designed to reduce the feature map size between these blocks. In particular, each transition layer contains a batch normalization operation, a 1×1 convolution, and a 2×2 average pooling layer. Moreover, a compression hyperparameter ϕ is also applied on transition layers to increase the architecture compactness by reducing the next block input features maps m to $\lfloor \phi m \rfloor$. Furthermore, notice that m directly depends on another hyperparameter k , called growth rate, that indicates the number of feature maps (i.e., filters) to be produced per layer. Intuitively, if H_l produces k feature maps, the l -th layer will have $k_0 + k * (l - 1)$ maps as input, where k_0 corresponds to the input image channels. Thus, by modifying k , it is possible to substantially change the number of network parameters. An overview of a densenet with dense blocks and transition layers is shown in Fig. 4.

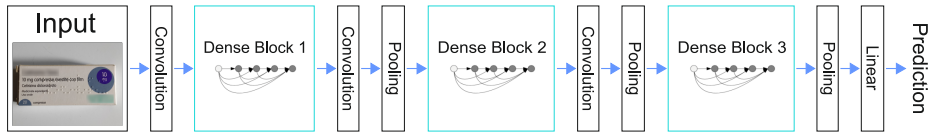


Fig. 4. Densenet architecture showing dense blocks interleaved by transition layers.

To apply the transfer learning paradigm and retain previous knowledge computed on the ImageNet dataset, all model weights are frozen apart from the linear layer used as a classifier component. The latter is then modified by changing its size to handle the right number of classes. Subsequently, the classifier is trained on the medicinal package classification task using the densenet extracted feature maps via the classical backpropagation algorithm and cross-entropy loss, thus exploiting prior knowledge via the frozen layers.

Finally, since the model receives frames from the camera feed in real-time, a λ threshold is applied on the confidence scores produced by the densenet to discard all classifications below it, to avoid showing the user information on uncertain recognitions. Indeed, by using this strategy, possible misclassification of objects with similar shapes, e.g., a generic box, are ignored by the application and only medicinal packages will be enhanced through the proposed AR interface.

3 Experiments

In this section, we first introduce the dataset used to test the mobile AR application, which was specifically collected to address the medicinal box classification task. Subsequently, implementation details for all of the described technologies are reported. Finally, a discussion on summarized performances obtained by the inference engine is presented.

3.1 Dataset

To correctly assess the presented model, 978 images for 63 distinct medicinal packages were collected from different sources such as Google and Bing images, as well as offline, directly through the phone camera. In addition, to reinforce the dataset difficulty, we ensured that among the 63 categories there were several distinct boxes presenting various similarities, e.g., shape or color scheme. Moreover, different lighting conditions, as well as distance and angles from the camera, were captured to further increase data variability. To train and test the model, the collection was divided using a stratified 10-fold cross-validation procedure using 80%/20% splits for the train and test sets, respectively. Notice that this approach retains the requested number of samples per class, thus ensuring there are enough samples for both training and test phases. Moreover, to further improve the model abstraction capabilities, a data augmentation strategy was devised by means of random horizontal flips and random rotations $\theta \in [-15, 15]$ degrees. Samples from the collected dataset are shown in Fig. 5.



Fig. 5. Medicinal boxes samples from the collected dataset.

3.2 Implementation Details

The presented mobile application was developed on an iOS mobile phone, i.e., iPhone 12 Pro. This device implements ARKit 5.0 and CoreML 4.1 frameworks, which enable, respectively, AR capabilities and neural network translation as well as its execution. This phone was selected due to both its ability to run the latest frameworks versions, as well as its hardware specifications, which allowed for a smooth real-time AR experience.

Concerning the transfer learning procedure, before implementing the application inference engine, the densenet was developed using the PyTorch framework and torchvision library, which contains an ImageNet pre-trained densenet version. In particular, we selected the densenet-121 model and modified its last linear layer to have 63 nodes, to match the dataset classes. Moreover, the default growth rate $k = 32$ and compression $\phi = 0.5$ were set for the architecture. A $\lambda = 0.85$ was also found to be a good confidence threshold to avoid uncertain classification showing in the AR interface. Regarding the training hyperparameters, the model was fine-tuned on the collected dataset for 100 epochs, using the SGD algorithm, with a learning rate lr set to 0.1, decreased by a factor of 10 at epochs 40, and 80, a weight decay of $5e-4$, and a Nesterov momentum of 0.9.

Finally, both training and experiments were performed using a 6-Core Intel i7 2.60GHz CPU with 32GB RAM and single GPU, i.e., a GeForce GTX 1070 with 8GB of dedicated RAM.

3.3 Performance Evaluation

In order to choose the best model parameters, ablation studies were performed on hyperparameters k and ϕ . Common classification metrics, i.e., accuracy, precision, recall, and f1-score, were used to assess each configuration that was tested using the aforementioned 10-fold cross-validation procedure.

Concerning the growth rate parameter k , the obtained results are summarized in Table 1. As shown, by increasing the number of filters generated by each convolutional layer, performances improve across all metrics, reaching up to an average 91.35% f1-score. More interestingly, using a low k number does not allow to represent and learn the input data distribution, resulting in consistent 30% gaps. For higher k values, instead, there are diminished performance returns. As a matter of fact, there is roughly a 0.02% difference between models using $k = 32$ and $k = 64$, indicating that enough information is already captured by the former value. What is more, the number of parameters and memory used at inference time increase superlinearly with respect to the growth rate k . Thus, since there are negligible performance gains, it is important to choose the correct k value to reduce the mobile device computational burden during inference; resulting in $k = 32$ as the better choice for the presented work.

Regarding the compression rate ϕ , results for various values are summarized in Table 2. As can be seen, reducing or increasing the extracted feature maps on transition layers via ϕ , has relatively little impact on the number of parameters, memory consumption, as well as all metrics. Nevertheless, using the default

Model	k	Params	Memory	Accuracy	Precision	Recall	F1-score
densenet-121	4	0.2M	0.9MB	61.13%	64.40%	61.13%	61.89%
densenet-121	8	0.6M	2.4MB	79.90%	80.74%	79.90%	80.09%
densenet-121	16	1.9M	7.7MB	89.07%	89.42%	89.07%	89.14%
densenet-121	32	7.0M	28.4MB	91.30%	91.51%	91.30%	91.33%
densenet-121	64	27.3M	109.7MB	91.32%	91.55%	91.32%	91.35%

Table 1. Ablation study on growth rate hyperparameter k . Results correspond to the 10-fold cross-validation scores average. For all networks, ϕ was set to 0.5.

0.5 value allows to achieve the best performances since first, it avoids losing too much information from the preceding dense block with respect to a lower 0.1 size; and second, it improves the model abstraction capabilities without incurring in possible overfitting scenarios, as opposed to the $\phi = 1.0$ case where performances begin to deteriorate.

Model	ϕ	Params	Memory	Accuracy	Precision	Recall	F1-score
densenet-121	0.1	6.5M	26.2MB	90.00%	90.28%	90.00%	90.06%
densenet-121	0.5	7.0M	28.4MB	91.30%	91.51%	91.30%	91.33%
densenet-121	1.0	7.7M	31.2MB	91.26%	91.51%	91.26%	91.31%

Table 2. Ablation study on compression hyperparameter ϕ . Results correspond to the 10-fold cross-validation scores average. For all networks, k was set to 32.

Although the ablation studies present interesting information, a better system overview can be provided by a confusion matrix, which is reported in Fig. 6. As expected, most predictions lie in the matrix diagonal, indicating that the model can correctly recognize all classes with a high accuracy. Furthermore, for a given box, misclassifications tend to concentrate on specific medicines, suggesting that there are similarities between those packages. As a matter of fact, this outcome can be confirmed by observing Fig. 7, which shows boxes misclassified by the presented densenet. As can be observed, the reported packages have similar sizes and colors but can have different product names, active substance weights or molecules. This indicates that while the system uses the entire box to recognize a medicine, it is still not able to accurately discriminate text; suggesting that the model can be further improved by refining its ability to classify written content, a task left as future work.

Finally, the densenet model with $k = 32$ and $\phi = 0.5$ was employed as inference engine inside the mobile application to enable stable real-time capabilities over a 30FPS video stream. Notice that the selected device achieved similar performances even with the more demanding $k = 64$ model, however since the AR interface showed several, albeit infrequent, frame drops, the less complex model was still the preferred choice to reduce the device burden.

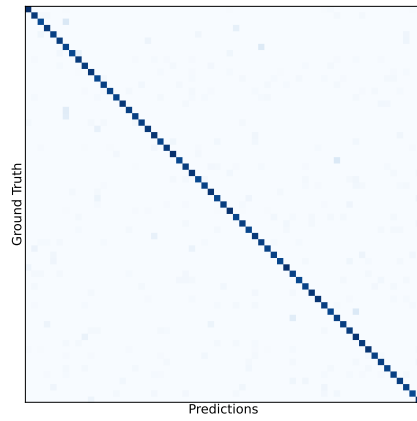


Fig. 6. Confusion matrix of a densenet-121 model with $k = 32$ and $\phi = 0.5$.

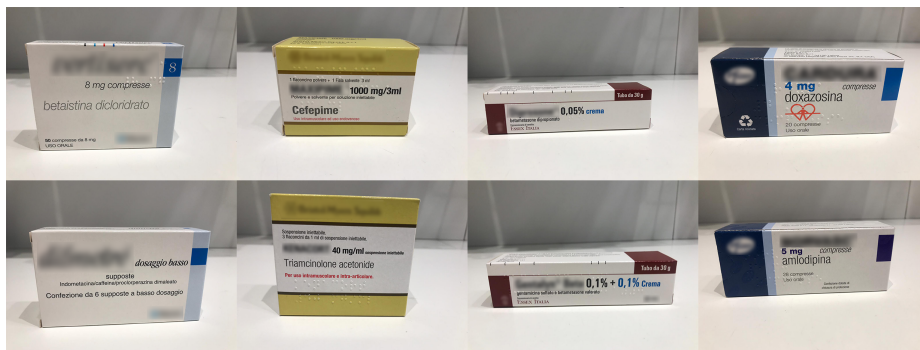


Fig. 7. Examples of misclassified medicine boxes.

4 Conclusions

In this paper we presented an AR mobile application that can classify medicinal boxes and show the user useful information, such as the posology or PIL, to help them using medicinals in a proper way. Extensive experiments were performed on a dataset specifically collected to address this task, and the best model configuration was selected to achieve real-time execution on the mobile device. Specifically, the chosen architecture, i.e., a densenet, obtains significant performances by exploiting the transfer learning paradigm, reaching up to 91.30% accuracy on 63 classes; highlighting the effectiveness of the proposed methodology.

Acknowledgments

This work was supported by the MIUR under grant “Departments of Excellence 2018–2022” of the Sapienza University Computer Science Department and the ERC Starting Grant no. 802554 (SPECGEO).

References

1. Aitamurto, T., Boin, J.B., Chen, K., Cherif, A., Shridhar, S.: The impact of augmented reality on art engagement: Liking, impression of learning, and distraction. In: *International Conference on Virtual, Augmented and Mixed Reality*. pp. 153–171 (2018)
2. Avola, D., Bernardi, M., Cascio, M., Cinque, L., Foresti, G.L., Massaroni, C.: A new descriptor for keypoint-based background modeling. In: *International Conference on Image Analysis and Processing (ICIAP)*. pp. 15–25 (2019)
3. Avola, D., Bigdello, M.J., Cinque, L., Fagioli, A., Marini, M.R.: R-signet: Reduced space writer-independent feature learning for offline writer-dependent signature verification. *Pattern Recognition Letters* **150**, 189–196 (2021)
4. Avola, D., Caschera, M.C., Ferri, F., Grifoni, P.: Ambiguities in sketch-based interfaces. In: *Annual Hawaii International Conference on System Sciences (HICSS)*. pp. 290b–290b (2007)
5. Avola, D., Cascio, M., Cinque, L., Fagioli, A., Foresti, G.L.: Human silhouette and skeleton video synthesis through wi-fi signals. *International Journal of Neural Systems* p. 2250015 (2022)
6. Avola, D., Cascio, M., Cinque, L., Fagioli, A., Foresti, G.L., Massaroni, C.: Master and rookie networks for person re-identification. In: *International Conference on Computer Analysis of Images and Patterns*. pp. 470–479 (2019)
7. Avola, D., Cascio, M., Cinque, L., Fagioli, A., Petrioli, C.: Person re-identification through wi-fi extracted radio biometric signatures. *IEEE Transactions on Information Forensics and Security* **Early Access**, 1–1 (2022)
8. Avola, D., Cinque, L., Di Mambro, A., Diko, A., Fagioli, A., Foresti, G.L., Marini, M.R., Mecca, A., Pannone, D.: Low-altitude aerial video surveillance via one-class svm anomaly detection from textural features in uav images. *Information* **13**(1), 2 (2021)

9. Avola, D., Cinque, L., Fagioli, A., Filetti, S., Grani, G., Rodolà, E.: Multimodal feature fusion and knowledge-driven learning via experts consult for thyroid nodule classification. *IEEE Transactions on Circuits and Systems for Video Technology* **1**, 1–8 (2021)
10. Avola, D., Cinque, L., Fagioli, A., Foresti, G.L., Massaroni, C.: Deep temporal analysis for non-acted body affect recognition. *IEEE Transactions on Affective Computing* **1**, 1–12 (2020)
11. Avola, D., Cinque, L., Fagioli, A., Foresti, G.L., Pannone, D., Piciarelli, C.: Bodyprint—a meta-feature based lstm hashing model for person re-identification. *Sensors* **20**(18), 5365 (2020)
12. Avola, D., Cinque, L., Fagioli, A., Foresti, G., Mecca, A.: Ultrasound medical imaging techniques: A survey. *ACM Computing Surveys (CSUR)* **54**(3), 1–38 (2021)
13. Avola, D., Cinque, L., Foresti, G.L., Marini, M.R.: An interactive and low-cost full body rehabilitation framework based on 3d immersive serious games. *Journal of Biomedical Informatics* **89**, 81–100 (2019)
14. Avola, D., Foresti, G.L., Cinque, L., Massaroni, C., Vitale, G., Lombardi, L.: A multipurpose autonomous robot for target recognition in unknown environments. In: *International Conference on Industrial Informatics (INDIN)*. pp. 766–771 (2016)
15. Avola, D., Foresti, G.L., Martinel, N., Micheloni, C., Pannone, D., Piciarelli, C.: Real-time incremental and geo-referenced mosaicking by small-scale uavs. In: *International Conference on Image Analysis and Processing (ICIAP)*. pp. 694–705 (2017)
16. Avola, D., Spezialetti, M., Placidi, G.: Design of an efficient framework for fast prototyping of customized human–computer interfaces and virtual environments for rehabilitation. *Computer Methods and Programs in Biomedicine* **110**(3), 490–502 (2013)
17. Baldini, G., Steri, G.: A survey of techniques for the identification of mobile phones using the physical fingerprints of the built-in components. *IEEE Communications Surveys & Tutorials* **19**(3), 1761–1789 (2017)
18. Freire-Obregón, D., Narducci, F., Barra, S., Castrillón-Santana, M.: Deep learning for source camera identification on mobile devices. *Pattern Recognition Letters* **126**, 86–91 (2019)
19. He, Z., Wu, L., Li, X.R.: When art meets tech: The role of augmented reality in enhancing museum experiences and purchase intentions. *Tourism Management* **68**, 127–139 (2018)
20. Huang, G., Liu, Z., Van Der Maaten, L., Weinberger, K.Q.: Densely connected convolutional networks. In: *IEEE Conference on Computer Vision and Pattern Recognition (CVPR)*. pp. 4700–4708 (2017)
21. Konig, A., Satt, A., Sorin, A., Hoory, R., Derreumaux, A., David, R., Robert, P.H.: Use of speech analyses within a mobile application for the assessment of cognitive impairment in elderly people. *Current Alzheimer Research* **15**(2), 120–129 (2018)
22. Mayo-Gamble, T.L., Mouton, C.: Examining the association between health literacy and medication adherence among older adults. *Health Communication* **33**(9), 1124–1130 (2018)
23. Petersen, M., Hempler, N.F.: Development and testing of a mobile application to support diabetes self-management for people with newly diagnosed type 2 diabetes: a design thinking case study. *BMC Medical Informatics and Decision Making* **17**(1), 1–10 (2017)
24. Petracca, A., Carrieri, M., Avola, D., Moro, S.B., Brigadoi, S., Lancia, S., Spezialetti, M., Ferrari, M., Quaresima, V., Placidi, G.: A virtual ball task driven

- by forearm movements for neuro-rehabilitation. In: International Conference on Virtual Rehabilitation (ICVR). pp. 162–163 (2015)
25. Rahmawati, E., Listyasari, M., Aziz, A.S., Sukaridhoto, S., Damastuti, F.A., Bachtiar, M.M., Sudarsono, A.: Digital signature on file using biometric fingerprint with fingerprint sensor on smartphone. In: International Electronics Symposium on Engineering Technology and Applications (IES-ETA). pp. 234–238 (2017)
 26. Ríos-Sánchez, B., Costa-da Silva, D., Martín-Yuste, N., Sánchez-Ávila, C.: Deep learning for face recognition on mobile devices. *IET Biometrics* **9**(3), 109–117 (2020)
 27. de Souza Cardoso, L.F., Mariano, F.C.M.Q., Zorzal, E.R.: A survey of industrial augmented reality. *Computers & Industrial Engineering* **139**, 106159 (2020)
 28. Tun, S.Y.Y., Madanian, S., Mirza, F.: Internet of things (iot) applications for elderly care: a reflective review. *Aging Clinical and Experimental Research* **33**(4), 855–867 (2021)
 29. Turkan, Y., Radkowski, R., Karabulut-Ilgü, A., Behzadan, A.H., Chen, A.: Mobile augmented reality for teaching structural analysis. *Advanced Engineering Informatics* **34**, 90–100 (2017)
 30. Zhao, F., Cao, Z., Xiao, Y., Mao, J., Yuan, J.: Real-time detection of fall from bed using a single depth camera. *IEEE Transactions on Automation Science and Engineering* **16**(3), 1018–1032 (2018)
 31. Zhuang, F., Qi, Z., Duan, K., Xi, D., Zhu, Y., Zhu, H., Xiong, H., He, Q.: A comprehensive survey on transfer learning. *Proceedings of the IEEE* **109**(1), 43–76 (2020)